

# Continuous-Wave Second-Harmonic Generation in Orientation-Patterned Gallium Phosphide Waveguides at Telecom Wavelengths

Konstantinos Pantzas  
C2N  
CNRS, Université Paris Saclay  
Palaiseau, FRANCE  
konstantinos.pantzas@c2n.upsaclay.fr

Sylvain Combrié  
Groupe de Physique  
Thales Research and Technology  
Palaiseau, FRANCE  
sylvain.combrie@thalesgroup.com

Alfredo De Rossi  
Groupe de Physique  
Thales Research and Technology  
Palaiseau, FRANCE  
alfredo.derossi@thalesgroup.com

Yoan Léger  
Institut FOTON  
CNRS, Université Rennes, INSA  
Rennes, FRANCE  
Yoan.Leger@insa-rennes.fr

Arnaud Grisard  
Groupe de Physique  
Thales Research and Technology  
Palaiseau, FRANCE  
arnaud.grisard@thalesgroup.com

Isabelle Sagnes  
C2N  
CNRS, Université Paris Saclay  
Palaiseau, FRANCE  
isabelle.sagnes@c2n.upsaclay.fr

**Abstract**—A new process to produce Orientation-Patterned Gallium Phosphide (OP-GaP) on GaAs with almost perfectly parallel domain boundaries is presented. Taking advantage of the chemical selectivity between phosphides and arsenides, OP-GaP is processed into suspended shallow-ridge waveguides. Efficient Second-Harmonic Generation from Telecom wavelengths is achieved in both Type-I and Type-II polarisation configurations. The highest observed conversion efficiency is  $200\% \text{ W}^{-1} \text{ cm}^{-2}$ , with a bandwidth of 2.67 nm in a 1 mm-long waveguide. The variation of the conversion efficiency with wavelength closely follows a squared cardinal sine function, in excellent agreement with theory, confirming the good uniformity of the poling period over the entire length of the waveguide.

**Index Terms**—nonlinear optics, gallium phosphide, second-harmonic generation

## I. INTRODUCTION

Quasi-phase matched (QPM) nonlinear frequency conversion in semiconductors requires the periodic reversal of the second-order susceptibility  $\chi^{(2)}$ , achieved through the periodic reversal of the semiconductor crystal. Using this approach, Orientation-Patterned Gallium Arsenide (OP-GaAs) has, for instance, successfully replaced Periodically Poled Lithium Niobate (PPLN) at wavelengths between 4  $\mu\text{m}$  and 12  $\mu\text{m}$ . Nevertheless, with a short-wavelength absorption edge in GaAs at 2  $\mu\text{m}$ , two-photon absorption becomes prohibitively high for SHG in OP-GaAs at telecom wavelengths. Another III-V semiconductor, gallium phosphide (GaP) has negligible two-photon absorption for wavelengths above 1  $\mu\text{m}$ , in addition to several other properties that make it alluring for nonlinear photonics: large  $\chi^{(2)}$  and  $\chi^{(3)}$  nonlinearities,

and a high transparency from 500 nm to 12  $\mu\text{m}$ . Moreover, GaP offers several technological advantages for Si Photonics, including a small lattice mismatch with Si (0.1 % at room temperature), and a high thermal conductivity. This slew of advantageous properties has prompted several groups to propose and develop OP-GaP crystals for bulk non-linear optics [1]. To date, however, little effort has been devoted to waveguide devices. The present work leverages earlier developments in OP-GaAs waveguides [2] to design and fabricate OP-GaP waveguides capable of continuous wave (CW) second harmonic generation (SHG) from 1.5  $\mu\text{m}$  lasers. A conversion efficiency of  $200\% \text{ W}^{-1} \text{ cm}^{-2}$  is demonstrated, the highest to our knowledge reported using this technology. This result paves the way for efficient integrated frequency converters, and enables the use of highly efficient silicon-based detectors for telecom-signal detection.

## II. WAVEGUIDE DESIGN AND FABRICATION

An air-clad, suspended, shallow-ridge waveguide design was chosen to demonstrate SHG at telecom wavelengths in OP-GaP. This design ensures a maximum overlap between the fundamental and second harmonic modes, while minimizing optical losses. The total height  $h$  of the suspended waveguide is 3  $\mu\text{m}$ , the etch-depth  $h_r$  is 1.6  $\mu\text{m}$ , and the width  $w$  of the ridge is 4.5  $\mu\text{m}$ . The index profile of this waveguide is shown in Figure 1a. Given these parameters, the relevant field distributions were computed and are represented in Figs. 1b and 1c. The TE and TM modes are shown to perfectly overlap. The effective indices for both modes as a function of wavelength were also computed (see Fig. 1d). Using these effective indices, the evolution of the QPM period  $\Lambda = k_{2\omega} - 2k_\omega$  with the wavelength was also calculated. The plot reveals that  $\Lambda$  needs to be between 4.6 and 5.6  $\mu\text{m}$

The present work has been supported by the French Renatech network and by the National Research Agency (ANR-17-CE24-0019). F. Talenti received funding from the European Union's Horizon 2020 Research and Innovation Program under the Marie Skłodowska-Curie grant agreement No. 814147.

for operation in the telecom window. Here, a QPM period of  $5.5\ \mu\text{m}$  was chosen. Using the above design parameters, OP-GaP waveguides were grown on OP-GaAs seed wafers, using a  $700\ \text{nm}$  thick  $\text{Al}_{0.85}\text{Ga}_{0.15}\text{As}$  etch-stop layer underneath the GaP membrane. To free this membrane, the first step is to etch  $5 \times 10\ \mu\text{m}$  apertures on the sides of the waveguide, all the way into the buried  $\text{Al}_{0.85}\text{Ga}_{0.15}\text{As}$  layer. These apertures serve as vias to suspend the waveguide in the final processing step. Then, the  $1.6\ \mu\text{m}$  deep by  $4.5\ \mu\text{m}$  wide waveguide is etched into the OP-GaP layer. Finally, the waveguide is suspended by selectively removing the  $\text{Al}_{0.85}\text{Ga}_{0.15}\text{As}$  using wet etching. After processing, the sample is cleaved, creating  $1\ \text{mm}$  waveguides.

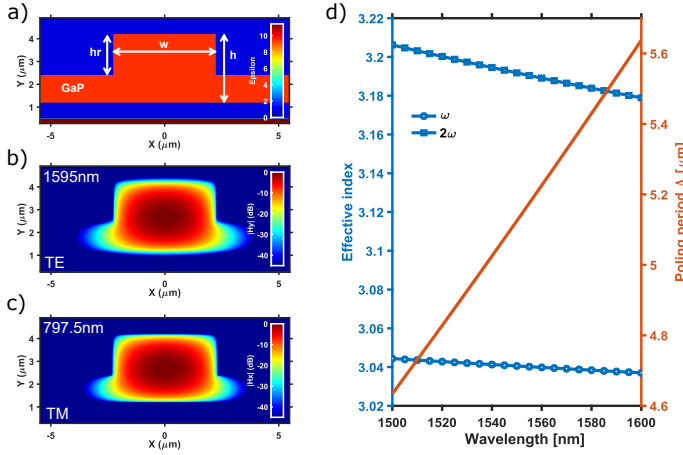


Fig. 1. a) index profile of the OP-GaP waveguide. (b) Calculated magnetic field distribution for the fundamental mode in transverse electric (TE) polarization and (c) for the SHG in transverse magnetic (TM) polarization. (d) Numerical calculations of effective indices for fundamental  $\omega$  and SHG  $2\omega$  modes. Also plotted is the QPM period  $\Lambda$  as a function of wavelength (right-hand axis).

### III. WAVEGUIDE CHARACTERIZATION

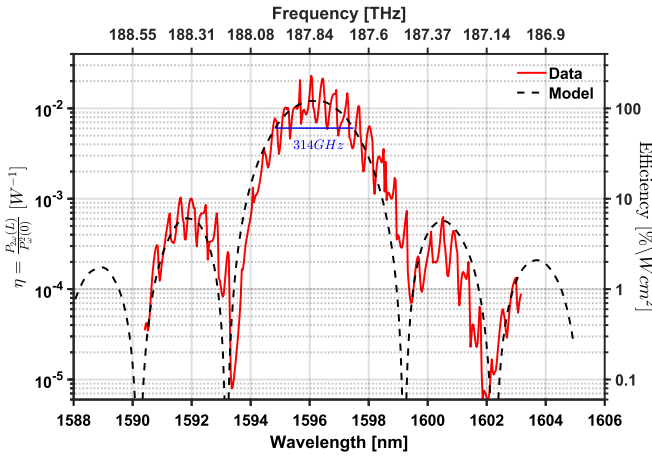


Fig. 2. Conversion efficiency as a function of wavelength. The red solid curve represents the experimental data. The black dashed curve is in good agreement with the model from Ref. [3].

Fig. 2b shows the conversion efficiency of the OP-GaP waveguides as a function of output wavelength. The peak efficiency reaches  $200\ \% \text{ W}^{-1} \text{ cm}^{-2}$ . The measured 3 dB bandwidth is  $2.67\ \text{nm}$ . The envelope of the conversion efficiency follows a squared cardinal sine function characteristic of the spectral acceptance of the SHG process. It is modulated by periodic fluctuations that are due to Fabry-Pérot interference. The envelope can be modelled following Reference [3]. This model takes into account propagation losses and expresses  $\eta$  as follows:

$$\eta = \frac{2\omega^2}{\epsilon_0 c^3} \frac{d_{\text{eff}}^2}{n_{\omega}^2 n_{2\omega}} L^2 \mathcal{H}\Gamma. \quad (1)$$

The conversion efficiency reported here is the highest to date for OP-GaP, several orders of magnitude higher than other reports in the literature for the same material and second-harmonic generation. This improvement is both due to the quality of the OP-GaP crystal, i.e. the very high domain fidelity, and confinement in the waveguide [4].

Nevertheless, the efficiency reported here is still significantly lower than that reported for waveguides fabricated in competing nonlinear materials, in particular PPLN [5] and OP-GaAs. A major discriminating factor here are the losses in the waveguide,  $7\ \text{cm}^{-1}$ . These are an order of magnitude higher than those reported for competing technologies and can still be significantly improved upon, as has been done in the past for technologically more mature III-V semiconductors, such as GaAs or InP.

### IV. CONCLUSION

We successfully fabricated the first air-clad, suspended, shallow-ridge OP-GaP waveguides designed for SHG at telecom wavelengths with record-high conversion efficiencies, proving the potential of these devices for future wavelength converters of telecom signals and paving the way towards efficient integrated nonlinear optics [6].

### REFERENCES

- [1] V. L. Tassev, S. R. Vangala, R. D. Peterson, M. M. Kimani, M. Snure, R. W. Stites, S. Guha, J. E. Slagle, T. R. Ensley, A. A. Syed, and M. I. V, "Heteroepitaxial growth of OPGaP on OPGaAs for frequency conversion in the IR and THz," *Optical Materials Express*, vol. 6, no. 5, pp. 1724–1737, 2016.
- [2] A. Grisard, E. Lallier, and B. Gérard, "Quasi-phase-matched gallium arsenide for versatile mid-infrared frequency conversion," *Optical Materials Express*, vol. 2, pp. 1020–1025, Aug 2012.
- [3] T. Pliska, D. Fluck, P. Günter, L. Beckers, and C. Buchal, "Linear and nonlinear optical properties of  $\text{KNbO}_3$  ridge waveguides," *Journal of Applied Physics*, vol. 84, no. 3, pp. 1186–1195, 1998.
- [4] A. P. Anthur, H. Zhang, Y. Akimov, J. R. Ong, D. Kalashnikov, A. I. Kuznetsov, and L. Krivitsky, "Second harmonic generation in gallium phosphide nano-waveguides," *Optics Express*, vol. 29, no. 7, pp. 10307–10320, 2021.
- [5] C. Wang, C. Langrock, A. Marandi, M. Jankowski, M. Zhang, B. Desiatov, M. M. Fejer, and M. Lončar, "Ultrahigh-efficiency wavelength conversion in nanophotonic periodically poled lithium niobate waveguides," *Optica*, vol. 5, no. 11, pp. 1438–1441, 2018.
- [6] K. Pantzas, S. Combré, M. Bailly, R. Mandouze, F. R. Talenti, A. Harouri, B. Gérard, G. Beaudoin, L. Le Gratiet, G. Patriarche, A. De Rossi, Y. Léger, I. Sagnes, and A. Grisard, "Continuous-wave second-harmonic generation in orientation-patterned gallium phosphide waveguides at telecom wavelengths," *ACS Photonics*, 05 2022.